J. Ocean Univ. China (Oceanic and Coastal Sea Research)
DOI 10.1007/s11802-016-2545-4
ISSN 1672-5182, 2016 15 (1): 93-106
http://www.ouc.edu.cn/xbywb/
E-mail:xbywb@ouc.edu.cn

On the Tectonic Problems of the Southern East China Sea and Adjacent Regions: Evidence from Gravity and Magnetic Data

SHANG Luning[1), 2), 3)], ZHANG Xunhua[2), 3), *], HAN Bo[2), 3)], and DU Runlin[3)]

1) *College of Marine Geosciences*, *Ocean University of China*, *Qingdao* 266100, *P. R. China*
2) *Function Laboratory for Marine Mineral Resource Geology and Exploration*, *Qingdao National Oceanography Laboratory*, *Qingdao* 266000, *P. R. China*
3) *Institute of Marine Geology*, *Ministry of Land and Resources*, *Qingdao* 266071, *P. R. China*

(Received November 25, 2013; revised April 16, 2014; accepted October 1, 2015)

Abstract In this paper, two sets of gravity and magnetic data were used to study the tectonics of the southern East China Sea and Ryukyu trench-arc system: one data set was from the 'Geological-geophysical map series of China Seas and adjacent areas' database and the other was newly collected by *R/V Kexue III* in 2011. Magnetic and gravity data were reorganized and processed using the software MMDP, MGDP and RGIS. In addition to the description of the anomaly patterns in different areas, deep and shallow structure studies were performed by using several kinds of calculation, including a spectrum analysis, upward-continuation of the Bouguer anomaly and horizontal derivatives of the total-field magnetic anomaly. The depth of the Moho and magnetic basement were calculated. Based on the above work, several controversial tectonic problems were discussed. Compared to the shelf area and Ryukyu Arc, the Okinawa Trough has an obviously thinned crust, with the thinnest area having thickness less than 14 km in the southern part. The Taiwan-Sinzi belt, which terminates to the south by the NW-SE trending Miyako fault belt, contains the relic volcanic arc formed by the splitting of the paleo Ryukyu volcanic arc as a result of the opening of the Okinawa Trough. As an important tectonic boundary, the strike-slip type Miyako fault belt extends northwestward into the shelf area and consists of several discontinuous segments. A forearc terrace composed of an exotic terrane collided with the Ryukyu Arc following the subduction of the Philippine Sea Plate. Mesozoic strata of varying thicknesses exist beneath the Cenozoic strata in the shelf basin and significantly influence the magnetic pattern of this area. The gravity and magnetic data support the existence of a Great East China Sea, which suggests that the entire southern East China Sea shelf area was a basin in the Mesozoic without alternatively arranged uplifts and depressions, and might have extended southwestward and connected with the northern South China Sea shelf basin.

Key words tectonics; southern East China Sea; Ryukyu trench-arc system; gravity anomaly; magnetic anomaly

1 Introduction

The area located between China's mainland and the Ryukyu Trench is a tectonically complex area that includes the relatively stable passive-type continental shelf and slope to the west and the active Ryukyu trench-arc-backarc basin system to the east. Several elongated tectonic units separated primarily by normal faults can be identified: from west to east, they are the Zhemin uplift belt, East China Sea shelf basin, Taiwan-Sinzi belt, Okinawa Trough and Ryukyu Arc (Liu, 1992; Hsu, 2001; Lin *et al.*, 2005). The above linear highs and depressions are oriented in NNE-SSW or NE-SW direction and are sub-parallel to each other in the northern part; but this orientation is disturbed in the south.

In the southern East China Sea and neighboring area, several ongoing tectonic processes can be observed. As a result of the collision between the Luzon Arc and Eurasian continent (Teng, 1990), the Taiwan orogen has been uplifting since the Pliocene, and the main mountain-building process at present has migrated southward to the middle and southern Taiwan (Teng, 1996). As a nascent backarc basin, the Okinawa Trough extends southward to the onshore Ilan Plain in northeastern Taiwan and has been suggested as propagating southwestward along with the post-orogeny collapse and backarc extension (Wang *et al.*, 2000; Huang *et al.*, 2012; Hou *et al.*, 2009; Lai *et al.*, 2009). Multi-channel seismic reflection data have revealed that the initial rifting of the southern Okinawa Trough can be traced to the earliest Pleistocene (Park, 1998; Wu *et al.*, 2007), which is relatively younger than the late Miocene age suggested for the middle and northern Okinawa Trough (Lee *et al.*, 1980; Kimura, 1985; Letouzey and Kimura, 1985; Sibuet *et al.*, 1987). However, the southern Okinawa Trough has rapidly evolved into a drifting stage, and the oceanic crust may have emplaced in the central graben, which is evidenced by seismic refraction (Hirata *et al.*, 1990), magnetic lineations (Kimura,

* Corresponding author. Tel: 0086-532-85755800
E-mail: xunhuazh@vip.sina.com

1985; Sibuet *et al.*, 1987) and lithology data (Li *et al.*, 1997; Ma *et al.*, 2004). The southern East China Sea shelf basin has a different evolutionary history from the northern region in the Mesozoic (Yang *et al.*, 2012a), and the basin structure was modified severely by the arc-continent collision, especially in the area west and north of Taiwan (Yang *et al.*, 2012c).

Our study area is located between 23˚–28˚N and 120˚–128˚E (Figs.1 and 2). Authors from Japan, France and China's Taiwan have studied the spectacular tectonic features and processes of the area and contributed much to our understanding of the geodynamics of the Ryukyu trench-arc-backarc system and Taiwan orogen. Studies conducted by authors from China's mainland have primarily focused on the shelf basin that is enriched with oil and gas resources, and most of the results have been published in Chinese.

As evidenced by previous studies, gravity and magnetic inversions are effective methods of performing tectonic analyses of the East China Sea (Jin *et al.*, 1983; Gao *et al.*, 2000, 2004; Han, *et al.*, 2007, 2010; Han, 2008; Jiang *et al.*, 2002; Hsu 2001; Lin *et al.*, 2005). In this paper, gravity and magnetic data from different sources are presented and analyzed. In addition to the description of the gravity and magnetic anomaly patterns, various qualitative and quantitative methods were used for the study of deep and shallow structures. Other work, especially those conducted by authors from the QIMG (Qingdao Institute of Marine Geology), are also summarized and integrated in the present work.

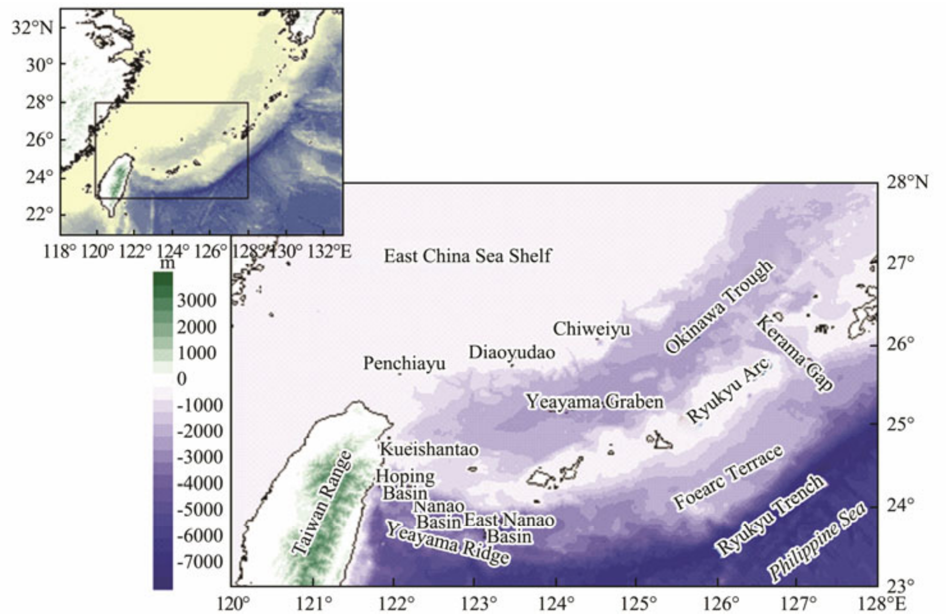

Fig.1 Bathymetry and topography of the study area; the major topographic units or features are labeled. The black rectangle in the small map indicates the location of the study area. Bathymetric data are from the Marine Geoscience Data System (http://www.geomapapp.org/ index.htm).

2 Data and Processing

Two main gravity and magnetic data sets were used in this paper. The first comes from the 'Geological-geophysical map series of China Seas and adjacent areas' database created by the QIMG. The gravity data consist of marine gravity data collected since the 1990s by several Chinese marine research institutes, such as the First and Second Institutes of Oceanography under the State Oceanic Administration, Guangzhou Marine Geological Survey, and Qingdao Institute of Marine Geology. The satellite gravity data are from the Scripps Institution of Oceanography (http://topex.ucsd.edu/www_heml/mar_grav.html). Magnetic data consist of marine magnetic data collected by the above Chinese marine research institutes and aeromagnetic data from the China Aero Geophysical Survey & Remote Sensing Center for Land and Resources. Both the gravity and magnetic data are corrected and integrated using the same parameters, such as a geodetic coordinate system, altitude datum, gravity datum and international geomagnetic reference fields. With grid spaces of approximately 5 km×5 km, this data set is adequate for studying the regional or sub-regional tectonics but not for performing a detailed analysis of the small structures, although analogous trials have been performed by previous authors (Li, 1987a, 1987b).

The second data set consists of gravity and magnetic data newly collected by *R/V Kexue III* of the IOCAS (Institute of Oceanology, Chinese Academy of Sciences) in 2011. The survey area is outlined by the gray double dot-dashed rectangle in Fig.2, and the positions of the survey lines are shown in Fig.10a. The main lines run in a N130˚E direction and are spaced 25 km apart; the cross-lines run in a N40˚E direction and are spaced 50 km apart. A KSS31M marine gravimeter and SeaSPY marine magnetometer were used for the gravity and magnetic measurements, respectively. Values were recorded every second. Both the reorganization and initial processing of the raw data were performed with the software MGDP and MMDP developed by Liu *et al.* (2011) and Bai *et al.* (2010) of the CUP (China University of Petroleum). Tidal, zero-drift and normal field corrections, Eotvos corrections, free-air anomaly corrections and Bouguer gravity anomaly corrections were applied to the gravity values, and normal field and diurnal variation corrections were applied to the magnetic values. Finally, the free-air anomaly, Bouguer anomaly and total-field magnetic anomaly were obtained. Limited to 121˚–126˚E, 26˚–28˚N, this data set covers the northwestern part of the study area (Fig.2) but was not integrated into the first data set because certain required parameters were missing. Compared to the first data set, the second set has a better resolution. Profiles with dense gravity and magnetic values can be extracted and used together with the synchronously collected seismic profiles for the tectonic inversion in the shelf region.

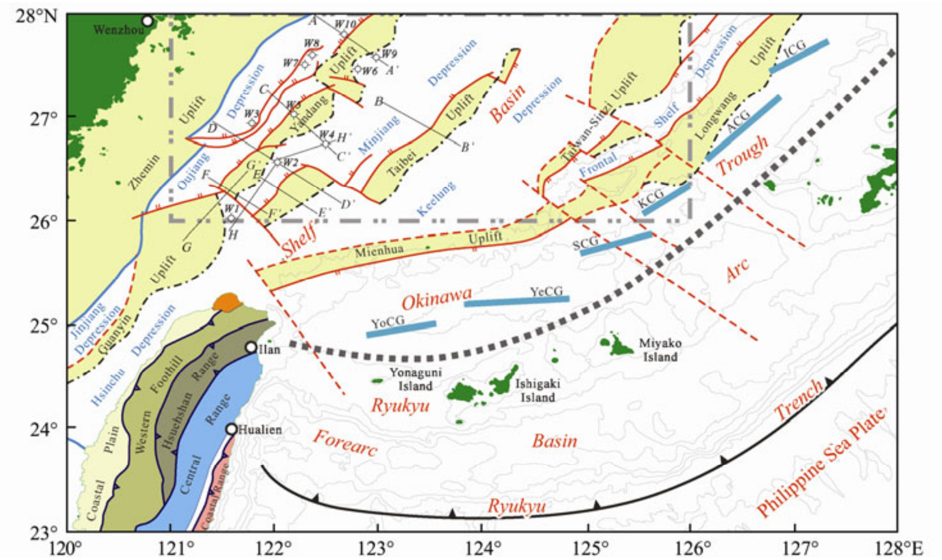

Fig.2 General structural map of the study area (modified from Zhao, 2004; Hsu, 2001). The red solid lines represent normal faults with hatchings on the downthrown side. The red dashed lines represent possible faults. Certain boundaries between different tectonic units are marked by black dash-dotted lines. Taiwan's structures are simplified from Huang *et al.* (2008), and the main thrust faults are marked by purple solid lines with the small triangle on the hanging sides. The basement highs in the shelf basin and Okinawa Trough areas are colored yellow, and the depressions have blue labels and are not colored. The survey area of 2011 is outlined by the gray double dot-dashed rectangle. The dark-gray dotted bar represents the Ryukyu volcanic front (Sibuet *et al.*, 1998). Blue bars in the Okinawa Trough show the position of the central grabens: YoCG–Yonaguni central graben, YeCG–Yaeyama central graben, SCG–Sakishima central graben, KCG–Kerama central graben, ACG–Aguni central graben and ICG–Iheya central graben. Light gray solid lines are isobaths. Locations of the wells in the shelf basin are denoted by small circles marked with short lines: W1-YCC-1X well, W2-FZ13-2-1 well, W3-Shimentan-1 well, W4-FZ10-1-1 well, W5-FZ2-1-1 well, W6-WZ23-1-1 well, W7-Mingyuefeng-1 well, W8-WZ15-1-1 well, W9-TB13-1-1 well and W10-W26-1-1 well.

The data processing and interpretation was performed with the software RGIS (Zhang, 2011), which was developed by the Development Research Center (DRC) of China Geological Survey (CGS). A spectrum analysis and upward-continuation were applied to the Bouguer anomaly to evaluate the deep crustal structures. The Moho depth was also calculated. The horizontal derivatives of the Bouguer anomaly and total-field magnetic anomaly were calculated to analyze the shallow structures. The depth and undulation of the magnetic basement were calculated using the spectrum analysis method. Most of the maps were generated by the software programs RGIS, Surfer or Grapher, but some were redepicted and polished by the software program CorelDRAW and provided as figures in this paper.

To determine the tectonic framework and better understand the tectonic processes in this area, additional published data, such as petrophysical data and seismic profiles, were also used, and the results of previous work (Gao *et al.*, 2000, 2004; Han *et al.*, 2007, 2010; Han, 2008; Jiang *et al.*, 2002; Hsu, 2001; Liu *et al.*, 2006) were taken into account.

3 Anomaly Patterns and Calculation Results

3.1 Free-Air Gravity Anomaly

3.1.1 East China Sea shelf

The East China Sea shelf area has a low free-air anomaly with values that generally range from 0–20 mGal (Fig.3). Several small enclosed areas with anomaly values of 0–20 mGal or −20–0 mGal are found in the western region. In the eastern margin of the shelf, the free-air anomaly is higher than 20 mGal, and certain areas are in excess of 40 mGal or even 60 mGal. The area enclosed by the 40 mGal isoline is approximately half the width of the 20 mGal area. The 20 mGal area extends southwestward to Penchiayu Island, but the 40 mGal area terminates near 124˚E and is severed near 125˚E by the lower anomaly, which corresponds to the submarine canyon. A triangular submarine platform with a flat surface and shallow water depth lies to the east of the canyon, and it is separated from the shelf by a wedge-shaped depression facing east. The platform has a high free-air anomaly over 100 mGal and is considered to be a residual terrane formed during the initial rifting of the Okinawa Trough (Wu *et al.*, 2004).

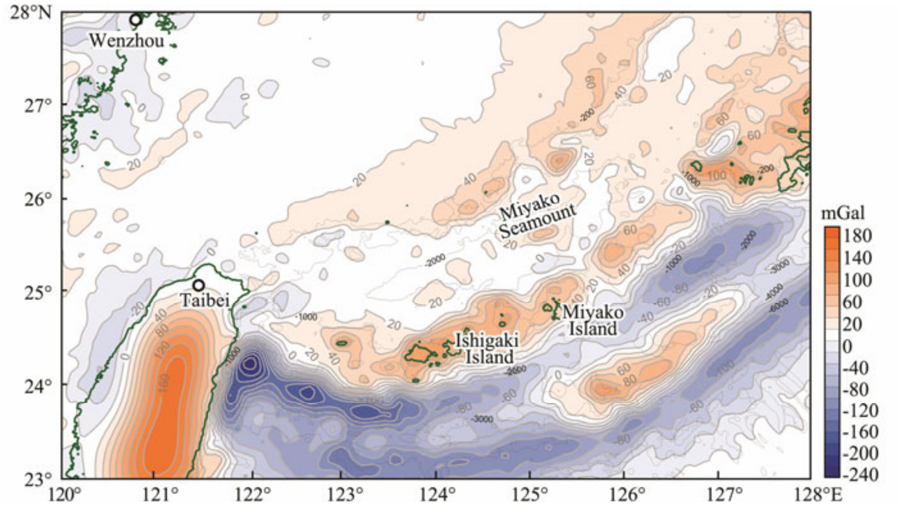

Fig.3 Free-air gravity anomaly of the study area. The shorelines are colored green. Black isobaths are superimposed on the map for comparison.

3.1.2 Okinawa Trough

The free-air anomaly in the Okinawa Trough can be divided into two parts that are bounded by the Miyako Seamount (Fig.3). The background values of the eastern and western regions are 20–40 mGal and 0–20 mGal, respectively. Two conspicuous anomalies are observed in the southern Okinawa Trough: the eastern high anomaly corresponds to the Miyako Seamount, and the western negative anomaly is located offshore of northeastern Taiwan. Similar to the platform to the north, the Miyako Seamount has also been suggested as a residual terrane (Kimura, 1985; Letouzey and Kimura, 1985; Sibuet *et al.*, 1987). The western negative anomaly may be related to the melting processes near the subducting slab edge (Lin *et al.*, 2004a, 2004b). Although the Okinawa Trough is a bathymetric basin that is generally deeper than −2000 m, its free-air gravity anomaly values are comparable to or even higher than the shelf area where the water depth is shallower than −200 m, this indicates that there are excessive masses in the deep lithosphere beneath the trough.

3.1.3 Ryukyu Arc and Ryukyu Trench

The free-air gravity anomaly of the Ryukyu Arc is higher than that of the Okinawa Trough. The anomaly is consistent with the topography and 20 mGal isoline that outlines the arc area. Values higher than 80 mGal generally correspond to the islands above the sea surface, and the highest values are over 100 mGal. The Ryukyu Trench has a negative free-air anomaly, and along the trench axis, the lowest values can reach −120 mGal.

3.1.4 Forearc area

The submarine topographic units of the forearc area between the Ryukyu Arc and Ryukyu Trench include the forearc terrace, basins, ridges and inner trench slope (Fig.1). Southeast of Miyako Island, a terrace is outlined by the −2000 m isobath between 125˚E and 127˚E, and the summit area is near the outer edge, which is shallower than −1000 m. The frontal slope break outside the terrace is obvious, trends NE-SW and is roughly parallel to the Ryukyu Arc. West of the terrace, the sea floor deepens westward and the forearc region can be divided into two belts that are both parallel to the arc and convex to the south. The inner belt consists of several forearc basins, including the Hoping, Nanao and East Nanao basins from west to east (Fig.1). The outer belt is the Yaeyama Ridge.

Although the bathymetry changes drastically in a latitudinal direction, the entire forearc region can still be summarized longitudinally as the forearc basins and forearc ridges, and the free-air anomaly pattern generally corresponds to the bathymetry. On the free-air gravity anomaly map, the southeastern part of the forearc terrace corresponds to an elliptical high anomaly area with a NE long axis. However, northeast of this area between 126˚ and 128˚E and out of the Kerama Gap, there is a low anomaly area that has shape, size and trend analogous with the first anomaly area. These two anomaly areas are left-laterally arranged and half overlapped, but the difference between the peak values can reach 200 mGal. Hereafter, the two anomalies are referred to as the 'free-air anomaly couple' or 'the couple', and their tectonic implications are discussed later in this paper. West of 125˚E, the free-air anomaly is regularly arranged and the ridge and basin have negative anomalies. The Yaeyama Ridge is outlined by the −100 mGal isoline. The anomaly of the basins decrease in a westward direction from −100 mGal south of Ishigaki Island to over −200 mGal in the Hoping Basin.

3.2 Bouguer Anomaly

The shelf area is characterized by a low positive Bouguer gravity anomaly, but there are some differences between the northern and southern regions (Fig.4). North of 26˚N, the background value is 20–40 mGal; however, 0–20 mGal entrapments of uneven size are distributed in the western region. South of 26˚N, most of the areas have values of 0–20 mGal, except the area with the negative anomaly west of Taiwan that corresponds to the foreland Hsinchu depression (Fig.2), which was formed by the Taiwan mountain building process that has occurred since the Pliocene (Zhao, 2004).

Compared with the shelf and Ryukyu Arc, the Okinawa Trough has a relatively high Bouguer anomaly. Therefore, a tremendous gradient zone that is subparallel to the trough formed on the eastern shelf margin and continental slope. The Bouguer anomaly of the Ryukyu Arc is approximately 100 mGal, but the elongated low anomaly areas between the Okinawa Trough and the Ryukyu Trench are centered on the forearc basin.

The Ryukyu Trench is characterized by a high positive anomaly over 320 mGal; in addition, the gradient zone northwest of the trench runs parallel to the trench-arc system but changes its direction abruptly to NNW west of 122˚E. The isolines south of the 120 mGal anomaly are obviously subparallel to each other, and the slope of the gradient zone is nearly constant. This coordination is disturbed north of the 120 mGal isoline. Because there is no remarkable change of the subducting angle, we suggest that the southern border of the arc crust may beneath the 120 mGal isoline. The Taiwan orogen has the most negative Bouguer anomaly in the study area, with minimum values of over −100 mGal. The seismic tomography results (Rau and Wu, 1995) have suggested that the crust thickened and the root may have formed under the orogen.

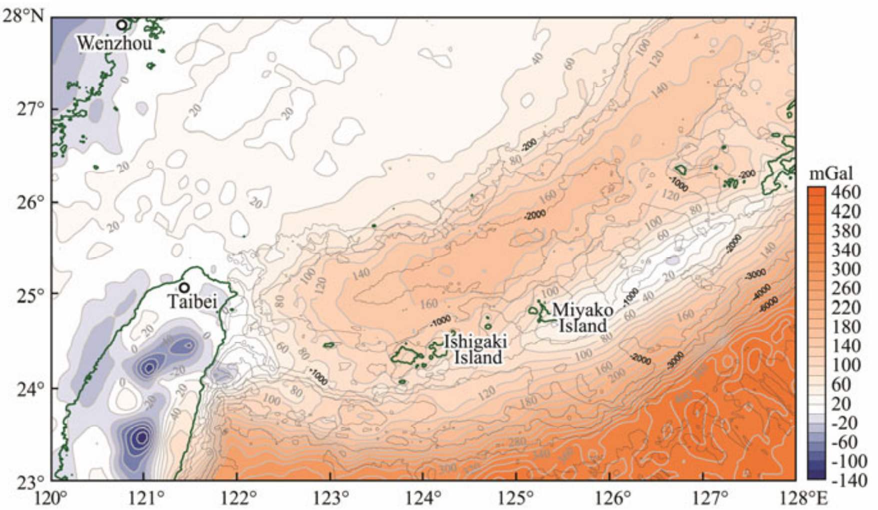

Fig.4 Bouguer anomaly of the study area. The shorelines are colored green. Black isobaths are superimposed on the map for comparison.

3.3 Magnetic Anomaly

The magnetic anomaly is shown in Fig.5. The Zhemin uplift belt located in the northwestern part of the study area (Fig.2) is characterized by high magnetic anomaly. On the mainland further west, Mesozoic and Cenozoic magmatic rocks are widely distributed in the Fujian and Zhejiang provinces (Yang *et al.*, 2012b), so we suggest that the high anomaly in the neritic area is related to the magmatic intrusions.

Generally, the NE-SW trending positive and negative anomalies with low amplitudes are distributed in the shelf basin area, but there are equiaxial anomalies with high amplitudes superimposed on the background field, suggesting that the magnetic basement is deeply buried but that certain magmatic intrusions exist, which are consistent with the igneous data (Yang *et al.*, 2012b), seismic profiles (Li *et al.*, 2012) and conclusions of some other authors (Jiang *et al.*, 2002).

The Taiwan-Sinzi belt is characterized by a high positive magnetic anomaly, but it is truncated by a NW trending low anomaly to the east of Chiweiyu Island. A high positive anomaly zone extends from Diaoyudao Island southeastward to Taibei, and this zone corresponds to the Northern Taiwan Volcanic Zone (NTVZ) (Chen *et al.*, 1995; Shinjo, 1998; Shinjo and Kato, 2000; Wang *et al.*, 1999). South of this high anomaly zone, there is a low positive anomaly area centered on the Ilan Plain, which is a triangular basin filled by thick sediments. The Ilan Plain has been suggested as a western extension of the Okinawa Trough that is undergoing a rifting process (Teng, 1996). Therefore, we suggest that the low anomaly of this area is related to the high heat flow and thick sediment cover.

The magnetic field in the Okinawa Trough can be divided into two parts by the NW-SE gradient zone east of the Miyako Seamount. The eastern region has low positive values and is centered on a large equiaxial negative area that corresponds to the active magmatic and hydrothermal area in the middle Okinawa Trough. The western region has a high positive anomaly over 60 nT, but it is truncated by the NW-SE magnetic low that is northwest of Ishigaki Island. A high anomaly lies to the north of the Yaeyama central graben. Moniliform high anomalies are distributed along the southern edge of the trough and correspond to a series of small sea knolls. Sibuet *et al.* (1998) suggested that these sea knolls belong to the Ryukyu volcanic front and extend to the Kuishantao Islet offshore of the Ilan Plain.

The Ryukyu Arc and forearc basin are magnetic quiet zones with an amplitude lower than 20 nT. However, the forearc ridge has a magnetic anomaly higher than 40 nT.

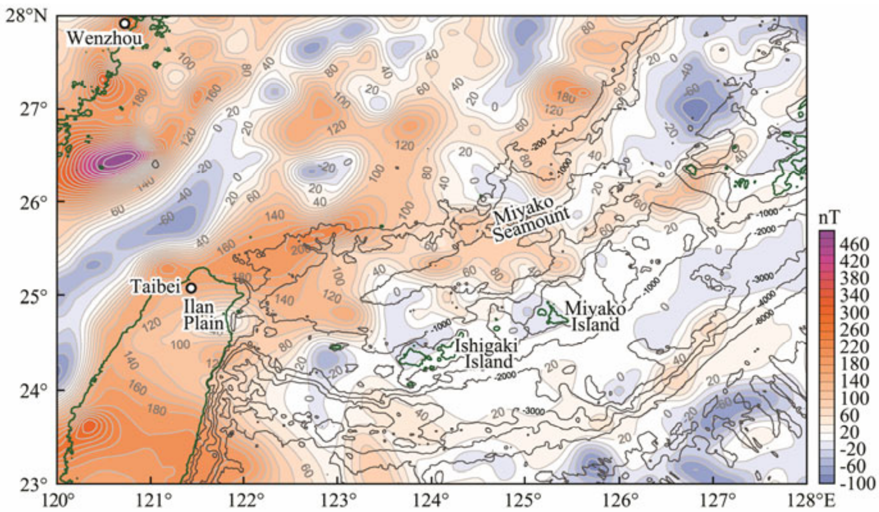

Fig.5 Magnetic anomaly of the study area. The shorelines are colored green. Black isobaths are superimposed on the map for comparison.

3.4 Moho Depth and Crust Thickness

As shown by previous work (Gao *et al.*, 2000; Han, 2008), wavelet analyses are efficient methods of decomposing gravity and magnetic data. In our work, the 4th order wave approximations were chosen as the raw data, and linear formulas were applied for the Moho depth calculation. Seismic detection results (Gao *et al.*, 2004, 2006) were considered as the constraints of the calculation results. The total crustal thickness was supposed to consist of the sedimentary layers, so it was calculated by eliminating the seafloor topography effects from the Moho depth.

The Moho depth and crustal thickness are shown in Figs.6 and 7, respectively. The crustal thickness of the study area is similar to the Moho depth in its distribution pattern, but it has a large gradient, which suggests that the Moho has mirror symmetry with the surface topography of the solid earth. Several main features can be observed. The mainland area has a normal continental crust thicker than 30 km. The shelf basin area has a relatively uniform crust thickness of 27–28 km, which is slightly thinner than the mainland area. As a result of the upwelling of the mantle, the crust of the Okinawa Trough has thinned drastically, and the thinnest area is less than 15 km and located near the Yaeyama central graben, which is also indicated by the seismic refraction survey results (Lee *et al.*, 1980; Hirata *et al.*, 1990). The crustal thickness of the Ryukyu Arc is over 20 km and close to that of the eastern edge of the continental shelf. The Philippine Sea Plate has a normal oceanic crust that is thinner than 7 km. The Taiwan orogen has a relatively thick crust compared to the surrounding area, and the maximum is over 31 km. Three dramatic gradient zones are observed: to the east of the shelf basin, in the Ryukyu forearc region and east of Taiwan. In general, our results are comparable to previous work.

If the disturbance of the Okinawa Trough and the Taiwan orogeny are eliminated, then the crustal thickness would have thinned eastward from China's mainland to the Philippine Sea; this point should be highlighted because it permits a better understanding of the tectonic evolution in this area.

3.5 Magnetic Basement Depth

The top surface of the magnetic basement is an important underground interface that significantly influences the magnetic anomaly pattern. In our work, the magnetic basement depth of the study area is calculated using the spectrum analysis method; the principle of this method was deduced and introduced by Han *et al.* (2010).

The magnetic basement depth is presented in Fig.8. Two subregions can be outlined in this area. One corresponds to the shelf region, and the other consists of the Ryukyu trench-arc-backarc basin system and Taiwan collision zone. The NE-trending magnetic basement highs and lows are distributed in the first subregion, but they do not necessarily correspond to the uplifts and depressions of the sedimentary basement after correlation with the tectonic map (Fig.2); this discordance is discussed later in this paper. The Taiwan-Sinzi belt displays a magnetic basement high that is shallower than 6 km and terminates near 124˚E. A sharp gradient zone inclining southeastward lies to the east side of the belt.

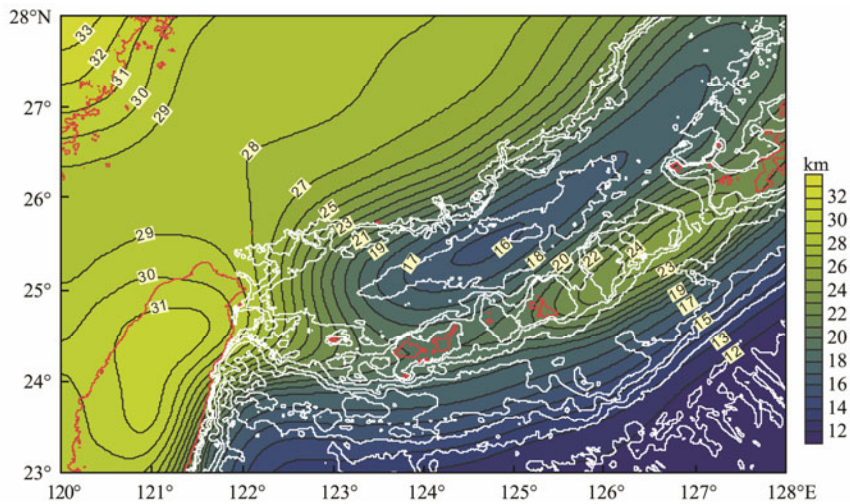

Fig.6 Moho depth of the study area. Contour interval is 1 km. The shorelines are colored red. White isobaths are superimposed on the map for comparison.

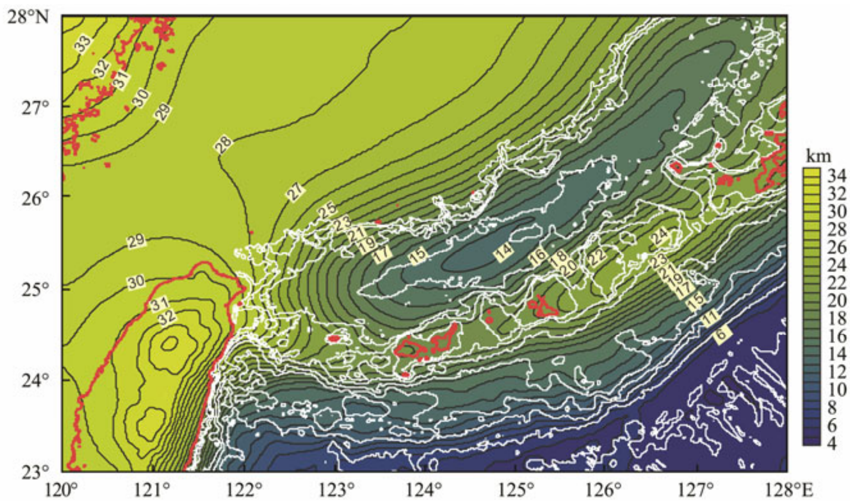

Fig.7 Crustal thickness of the study area. Contour interval is 1 km. The shorelines are colored red. White isobaths are superimposed on the map for comparison.

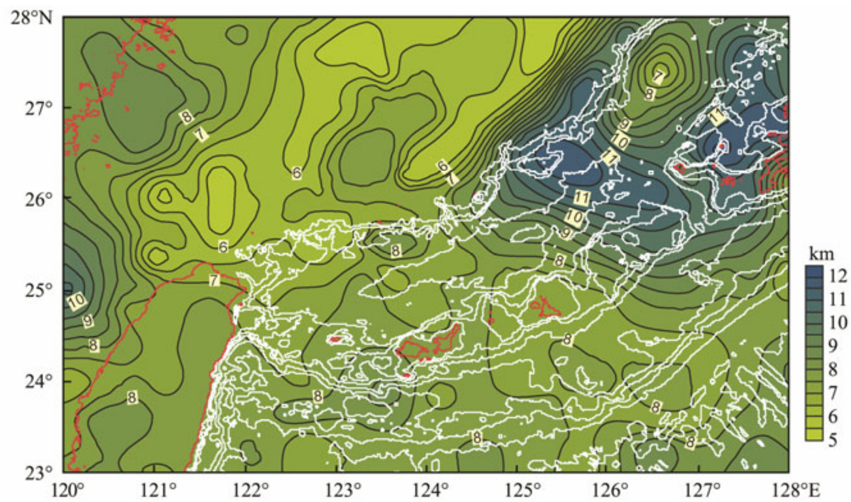

Fig.8 Top surface depth of the magnetic basement. Contour interval is 0.5 km. The shorelines are colored red. White isobaths are superimposed on the map for comparison.

The magnetic basement undulation of the second subregion is complex and influenced by multi-stage tectonism and magmatism; a clear regularity is difficult to discern based on solitary factor analyses. A sharp gradient zone inclining northeastward lies to the northeast side of Miyako Island and separates this subregion into two parts. The basement depth of the southwestern part is relatively stable, with placid variations mainly between 6 km and 8 km. In the northeastern part, however, the basement depth changes drastically in three encircled areas, including two basement lows trending NW-SE and NE-SW and one equiaxial basement high that corresponds to the hydrothermal area in the middle Okinawa Trough.

This calculation is only based on magnetic data, and the results have not been constrained or modified. However, correlations with the seismic and well data have the potential to facilitate determining and solving certain problems; in addition, the calculation results could be used for evaluations.

4. Discussions

4.1 Taiwan-Sinzi Belt

The Taiwan-Sinzi belt is a basement high located at the east margin of the East China Sea shelf. Before the opening of the Okinawa Trough, this belt was integrated with the Ryukyu belt and formed the outer ridge of the East China Sea, which was produced by the subduction of the Pacific Plate underneath the Eurasian Plate in the Mesozoic. In the Paleogene, this ridge emerged above sea-level, separated the rifting basins to the west and subduction zone to the east and provided enormous amounts of clastic material for the basins, which was shown by a heavy mineral analysis of sedimentary rocks in the Xihu Depression (Wang *et al.*, 2012). The eastern portion of the outer ridge, the Ryukyu belt, had drifted eastward with the opening of the Okinawa Trough since the middle-late Miocene and formed the Ryukyu Arc. The Taiwan-Sinzi belt, however, has submerged and been overlaid by thin Quaternary and Neogene strata (Gao *et al.*, 2004, 2006).

Without dramatic changes in the bathymetry, the relatively high free-air anomaly corresponding to the Taiwan-Sinzi belt terminates south of Chiweiyu Island. Further south, anomalies higher than 40 mGal can hardly be found, suggesting a deep basement. The free-air anomaly data also show that the Taiwan-Sinzi belt is truncated by the submarine canyon east of Chiweiyu Island. The Bouguer anomaly of the Taiwan-Sinzi belt is comparable to the Ryukyu Arc, and the crust thicknesses of the two belts are close but slightly thinner than the shelf area. Thus, it can be inferred that before the subduction in the Mesozoic, these two belts were part of the passive East Asian continental margin with a transitional crust formed by previous rifting.

Compared to the magnetic quiet zone of the Ryukyu Arc, the Taiwan-Sinzi belt has a higher magnetic anomaly. The calculation results show that the magnetic basement of this belt is shallow, suggesting that the pre-existing transitional crust has been intruded by magma. High-amplitude, short-wavelength anomalies in magnetic profiles suggest that these intrusions are mainly composed of intermediate or basic rocks, which has also been shown by the profile inversion results (Zhao, 2004; Gao *et al.*, 2004, 2006). It is noteworthy that the high magnetic anomaly that runs along the continental margin is truncated by a NW-SE trending low anomaly near Chiweiyu Island. South of this low anomaly, the NEE-SWW trending high anomaly northeast of Taiwan corresponds to the Northern Taiwan Volcanic Zone, which was formed by the magmatism related to the post-collisional collapse and extension of the Okinawa Trough (Shinjo, 1998; Wang *et al.*, 1999). Thus, the Taiwan-Sinzi belt terminates near Chiweiyu Island.

On the other side of the Okinawa Trough at the Ryukyu volcanic front, the Tokara volcanic chain terminates near Kume Island, which is located at a position close to the southern end of the Taiwan-Sinzi belt. South of Kume Island, a series of small sea knolls have been suggested as being a part of the Ryukyu volcanic front (Sibuet *et al.*, 1998), but this is still controversial. Therefore, we suggest that the magmatism of the Tokara volcanic chain inherited the volcanism of the Taiwan-Sinzi belt, and the present Taiwan-Sinzi belt partly consists of the relic volcanic arc formed by the opening of the Okinawa Trough. It can also be inferred that a large discontinuity perpendicular to the trough developed near Chiweiyu Island. East of this discontinuity, the evolutionary processes of the middle and northern Okinawa Trough are similar but different from the southern portion.

4.2 Miyako Fault Belt

Two groups of faults have developed in and around the Okinawa Trough. One group is parallel to the trough and mostly includes normal faults. The other group trends from the N-S to NW-SE, which is perpendicular to the trough; therefore, this group has been suggested to be strike-slip faults. The faults of the second group are traceable geographically and visible topographically, and they are closely related to the submarine canyons (Zhao *et al.*, 2009) on the continental slope, bathymetry changes in the trough and isobath bendings of the arc slop.

Most of the NW trending faults are considered to have extended northwestward into the shelf area, but accurate positioning is obscured because of the thick shielding sediments. In the shelf basin, dextral strike-slip faults that offset the NE trending structural belts display flower structures on the seismic profiles. These faults may be the western counterparts of the NW trending faults in the Okinawa Trough, but the relationship between these two features requires further discussion.

One of the most important NW trending fault belts is the Miyako fault belt located east of Miyako Island. Based on the gravity and seismic reflection data, Li (1987b) has pointed out that the fault belt extends from the Ryukyu Trench to the shelf basin or even onshore China's mainland. Through equivalent magnetization calculations, Hsu (2001) has suggested that the NW-SE trending Miyako-Yandang high magnetization zone is a significant tectonic boundary that terminates the southward extension of the Taiwan-Sinzi belt, transfers different stress fields and separates different tectonic evolutionary regions on the two sides.

On our total-magnetic field map, a high anomaly belt consisting of a series of moniliform high anomalies can be observed between Miyako Island and Wenzhou. East of this belt is a discontinuous gradient zone with opposite inclinations in different segments. In the Okinawa Trough, this gradient zone can also be observed and is shown on a detailed magnetic map (Liu *et al.*, 2006). Pole-reduction and 30 km upward continuation results have revealed that the gradient zone separates the NE direction anomalies to the northeast and NW direction anomalies to the southwest, and it has been suggested as corresponding to a large tectonic feature in the crust (Liu *et al.*, 2006).

First- and second-order derivatives of the magnetic anomalies have been calculated following an orientation of N45˚E. A series of discontinuous linear highs and lows can be observed between Miyako Island and Wenzhou (Fig.9). We propose that these linear features are related to the Miyako fault belt. Through correlations with the magnetic anomaly map and the first-order and second-order derivatives maps, the positions of the faults are marked.

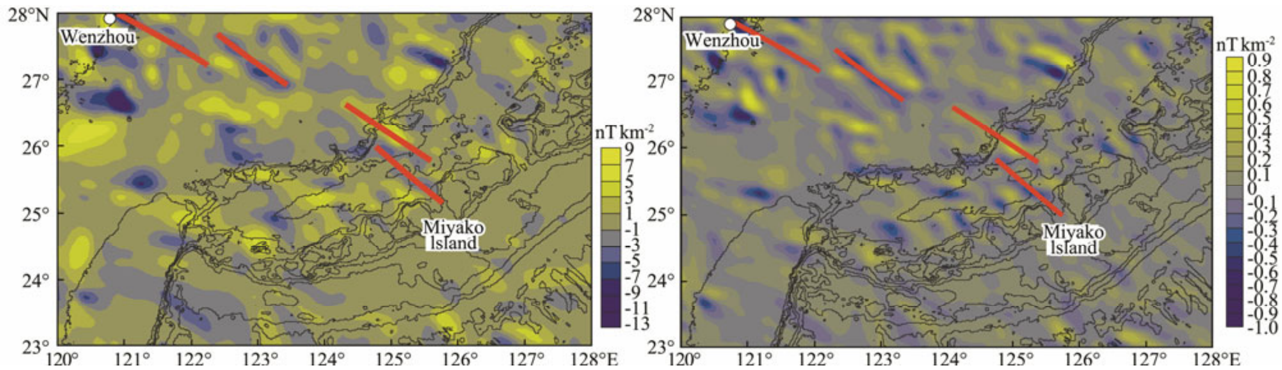

Fig.9 (a) A N45˚E-oriented horizontal first-order derivative of the magnetic anomaly. (b) A N45˚E-oriented horizontal second-order derivative of the magnetic anomaly. Different segments of the Miyako fault belt are marked by thick red solid lines.

As shown by the geological and geophysical data, the rifting and basin formation process in the East China Sea area has been migrating eastward since the Paleogene. During this migration, the NW trending faults played important transitional roles between different velocities and stress fields. Although the Miyako fault belt was submerged under thick sediments that are currently in the shelf basin and only detectable in pre-Pliocene strata and the basement (Li, 1987a, 1987b), it is reasonable to suggest from its discontinuous arrangement that the southeastward propagation of the fault was not gradual but mutational and that the rifting process continually 'jumped' eastward.

4.3 Forearc Tectonics

As previously described, the free-air gravity anomaly couple is a conspicuous feature in the forearc region (Fig. 3). On the Bouguer anomaly map, the NE section of the couple corresponds to a low anomaly area but has a larger size and extends westward to 125˚E. However, the SW section of the couple is located in a gradient zone with values that increase southeastward, which is consistent with other parts of the forearc region. Ishihara and Murakami (Honza, 1976) previously indicated that this region is a magnetically quiet zone where absolute values do not exceed 50 nT. On our magnetic anomaly map, however, a pair of anomalies can still be observed with lower and higher anomalies that correspond to the NE and SW parts of the couple, respectively. On the detailed magnetic map published by Hsu *et al.* (1996), this coupling is even more distinct.

A tectonic explanation of the couple has been provided by several authors, who suggest that the SW section with a high anomaly is an accretional forearc ridge, and the sediments from the west were dammed by the ridge and accumulated to form a forearc basin to the west (Shimajiri Depression). However, Hsu *et al.* (1996) suggested that the SW section with the high anomaly corresponds to an exotic terrane called the 'Gagua Terrane', which is the forehead of the tadpole-shaped paleo-Gagua ridge that emplaced on the Ryukyu Arc with the NW movement of the Philippine Sea Plate. Because of the high buoyancy of the Gagua Terrane, this segment of the trench migrated southeastward, and the fossil trench northwest of the terrane became a forearc basin that may have corresponded to the low anomaly area of the couple.

The OBS profiles reveal a surface low of the 5.6–6.0 km s^{-1} upper crust layer near the center of the low free-air anomaly region and show that the subducted oceanic crust and Moho are also downward bended (Kodaira *et al.*, 1996). However, the NW-SE trending multi-channel seismic reflection profile that runs across the high anomaly area does not reveal obvious undulations of the basement (Park, 1998). The NWW-SEE seismic reflection profile that runs across the low anomaly region reveals that the sediment thickness is greater than 7 km in the depression and that the subsidence center lies on the edge of the middle and lower crust; the P-wave velocities of these two layers are 6.1–6.9 km s^{-1} and 6.9–7.1 km s^{-1}, respectively. However, east of the depression, only 5.0–6.0 km s^{-1} of the upper crust is underlain by the subducting Philippine Sea Plate (Gao *et al.*, 2004). The magnetic inversion results from the same profile suggest that the magnetization of the basement underneath the depression is apparently different from that on the east side but resembles the Ryukyu Arc on the west side (Gao *et al.*, 2004).

In the western part of the forearc region, the Yaeyama Ridge is an accretionary wedge that is revealed by wide-angle seismic profiles (Klingelhoefer *et al.*, 2012). Although the forearc basins are supplied by abundant sediments from the nearby Taiwan orogeny, they are still in starvation and remarkably deeper than the Yaeyama Ridge. Compared to the west, the couple region is shown to be a relatively flat terrace that is shallower than −2000 m. Because such a large volume of sediments in the forearc basin cannot be supplied solitarily by the Ryukyu Arc, we suggest that the main infilling process had finished before the opening of the Okinawa Trough, when the sediments from China's mainland could be transported here. Therefore, the tectonic implication of the free-air gravity anomaly couple remains controversial and additional work should be done.

The inner slope of the trench becomes gentler in a westward direction; however, west of the Gagua Ridge, the accurate position of the trench is obscured, and certain authors have suggested that the present trench runs along the forearc basins (Hsu *et al.*, 1996). The Bouguer anomaly and wide-angle seismic profiles (Klingelhoefer *et al.*, 2012) all suggest that the trench runs south of the Yaeyama Ridge and the three forearc basins, the Hoping, Nanao, and East Nanao basins are underlain by an arc-type crust. Based on the OBS profiles, multi-channel seismic reflection profiles and gravity modeling, Wang *et al.* (2004) established the 3D structure of the southernmost Ryukyu subduction zone and suggested that the forearc basins and the rises that separate them are associated with the crust buckling, which resulted from increasing westward lateral compression as a result of the oblique subduction of the Philippine Sea Plate and collision with the Luzon Arc near the northwestern edge of the forearc region.

4.4 Tectonics of the Shelf Basin

The magnetic profiles (Fig.10b) reveal that the two NE-SW trending belts with high-amplitude short-wavelength anomalies located at the western and eastern edges of the continental shelf correspond to the Zhemin uplift and Taiwan-Sinzi belt, respectively, where the Mesozoic and/or Cenozoic igneous rocks are shallow buried. Most of the shelf basin area is characterized by low-amplitude long-wavelength anomalies that were generated by deep-buried metamorphic rocks or intermediate-acid igneous rocks.

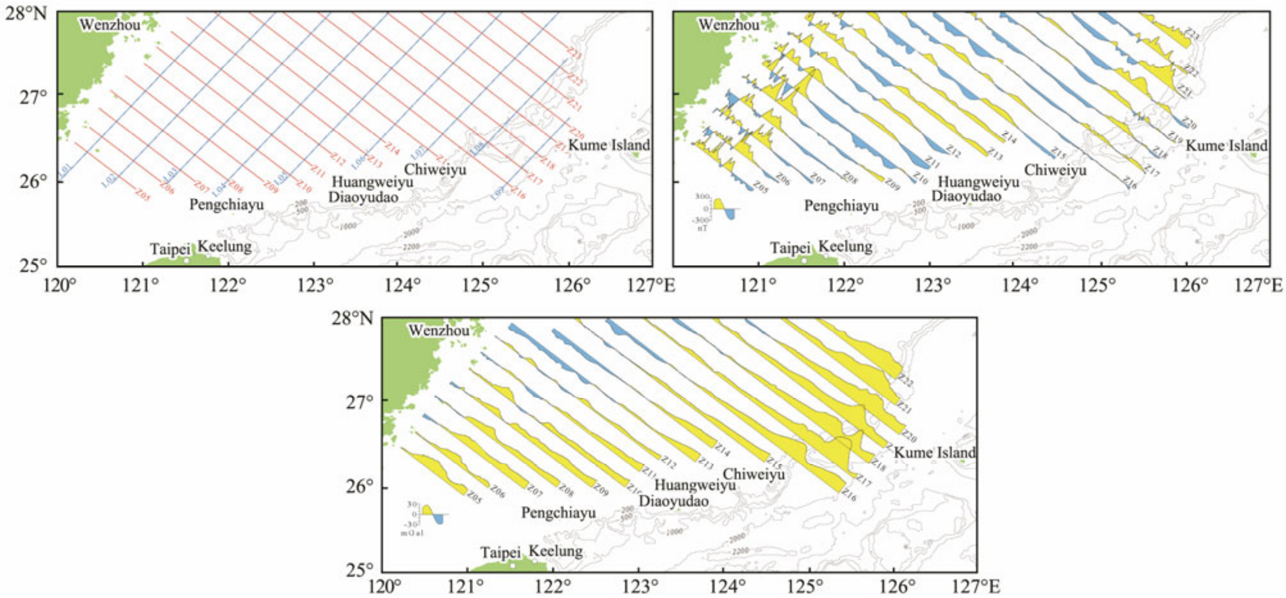

Fig.10 Magnetic and gravity anomalies of the 2011 data set. The anomalies are plotted at right angles to the ship tracks. (a) Locations of the survey lines; the main lines are colored red, and cross-lines are colored blue. (b) Magnetic anomaly profiles. (c) Free-air gravity anomaly profiles.

The well data from the shelf basin reveal that the basement under the Cenozoic sediments is composed of Mesozoic strata and pre-Sinian metamorphic rocks (Liu *et al.*, 2007). Because of the shallow penetration of wells and seismic reflection profiles, the Mesozoic strata overlain by the thick Cenozoic rocks are poorly understood. In the southern Minjiang depression, over 2000 m of Mesozoic strata are penetrated by the FZ13-2-1 and FZ10-1-1 wells, and it is divided into four formations (ascending order): the Fuzhou Formation, Yushan Formation, Minjiang Formation and Shimentan Formation (Liu *et al.*, 2007). The former three formations are composed of clastic rocks, but the Shimentan Formation is primarily composed of magmatic and pyroclastic rocks. The dating results show that this formation was formed in the Maastricht period of the Late Cretaceous. The seismic profiles reveal that the Mesozoic strata is widely distributed in the southern shelf basin and well-preserved in depressions with a maximum thickness of over 5000 m; however, the Mesozoic strata is thinned or even absent in the uplifts where the Cenozoic strata directly overlies the pre-Sinian basement.

Because the magnetic susceptibility of the magmatic rocks is higher than that of the metamorphic rocks, which in turn have a higher susceptibility than the sedimentary rocks, the magnetic anomaly intensity should follow the sequence of magmatic rock > metamorphic rock > sedimentary rock. If the influence of the magmatic rocks is excluded, the uplifts with a shallow-buried metamorphic basement should have a higher magnetic anomaly, shallower magnetic basement and higher free-air anomaly than the depressions; however, this is not the case. By correlating the structural map that was compiled by previous authors (Zhao, 2004) with the results from this study, we determined that the Taibei uplift has a high positive magnetic anomaly and shallow magnetic basement, whereas the other two uplifts, the Guanyin uplift and Yandang uplift, are characterized by low positive or negative magnetic anomalies without an obvious magnetic basement high. In contrast, the southern Minjiang Depression and western Keelung Depression are both characterized by high magnetic anomalies. Thus, we suggest that the Cretaceous igneous rocks are the main factor influencing the magnetic anomaly pattern in the shelf basin. On the free-air anomaly map (Fig.3 and Fig.9b), the Yandang uplift displays a high anomaly and the Guanyin uplift has a slightly higher anomaly than the neighboring Jinjiang depression, but the Taibei uplift displays no obviously anomaly.

Newly acquired and reprocessed seismic data (Li *et al.*, 2012) have provided some answers to the above questions. The basement structures and stratigraphic contact relationships can be elucidated through a correlation with the profiles that are perpendicular to the main tectonic trend (Fig.11). The metamorphic basement is shallow buried and directly overlain by Cenozoic strata in the northern Yandang uplift, but it deepens southward with thicker overlying Mesozoic strata. The Taibei uplift consists of several magmatic intrusions that were formed in late Yanshan tectonic period. The Guanyin uplift is overlain by a thick Mesozoic sedimentary layer that can be correlated with the layer in the Jinjiang Depression. Based on the seismic data, Li *et al.* (2012) proposed the existence of a Mesozoic Great East China Sea, which suggests that in the Mesozoic period, the Guanyin uplift and Taibei uplift did not exist and that the Yandang uplift was composed of three small discontinuous heaves. Therefore, different from the Cenozoic period, the entire southern East China Sea shelf area displayed a continuous basin without alternatively arranged uplifts and depressions in the Mesozoic, and the area may have been linked southwestward with the northern South China Sea shelf basin.

Integrating the seismic and well data, we conclude that because of the differential uplifting and subsidence in the Cenozoic, the pre-existing Mesozoic strata were preserved in depressions but eroded on the uplifts or intruded by magma. A discrepant thickness and composition of the remnant Mesozoic strata are important factors that influence the gravity and magnetic anomalies and decouple the magnetic basement from the acoustic basement, especially in the Yandang, Taibei and Guanyin uplifts.

5 Conclusions

Both old and newly collected magnetic and gravity data have been reprocessed for the purpose of tectonic studies in the southern East China Sea and Ryukyu Trench-Arc area from 23˚–28˚N and 120˚–128˚E. In addition to the description of the anomaly patterns, several calculations have been performed, such as for the Moho depth and top surface depth of the magnetic source. Based on the above results, several tectonic problems in the study area, which are still in debate, have been discussed and new perspectives have been proposed.

The crust thinned beneath the Okinawa Trough and thickened in the Taiwan orogen as a result of the backarc extension and arc-continental collision, respectively. These two features were superposed on the continental margin and obscured the pre-existing eastward thinning tendency of the crust.

The Taiwan-Sinzi belt is characterized by a high free-air anomaly, high magnetic anomaly and shallow magnetic basement, and it is terminated by the NW-SE trending Miyako fault belt near Chiweiyu Island and does not extend from Kyushu to Taiwan, as suggested by authors in the past. The shelf margin between the Taiwan and Miyako fault belt is covered by thick sediments, and the basement is deep buried; however, volcanic intrusions and extrusions developed and generated the high magmatic anomaly area northeast of Taiwan. The Taiwan-Sinzi belt northeast of Chiweiyu Island contains the relic volcanic arc formed by the splitting of the paleo volcanic arc as a result of the rifting of the Okinawa Trough, and its present counterpart may be the Tokara volcanic chain.

As an important tectonic boundary, the position of the Miyako fault belt has been poorly defined after its northwestward extension into the shelf basin. Through derivative calculations of the magnetic data, we suggest that the fault belt extends northwestward to Wenzhou and consists of several discontinuous segments that slightly overlap, which indicates a sudden rather than gradual southeastward migration of the rifting process since the late Mesozoic.

The Bouguer anomaly pattern suggests that the eastern border of the arc crust may run along the 120 mGal isoline or in the vicinity. First proposed by Hsu *et al.* (1996), the gravity and magnetic features suggest that the forearc terrace may have been topographically underlain by an exotic terrane that collided with the Ryukyu Arc during the subduction of the Philippine Sea Plate. The structural pattern of the westernmost part of the forearc region is mainly a result of the oblique subduction of the Ryukyu slab and arc-continent collision.

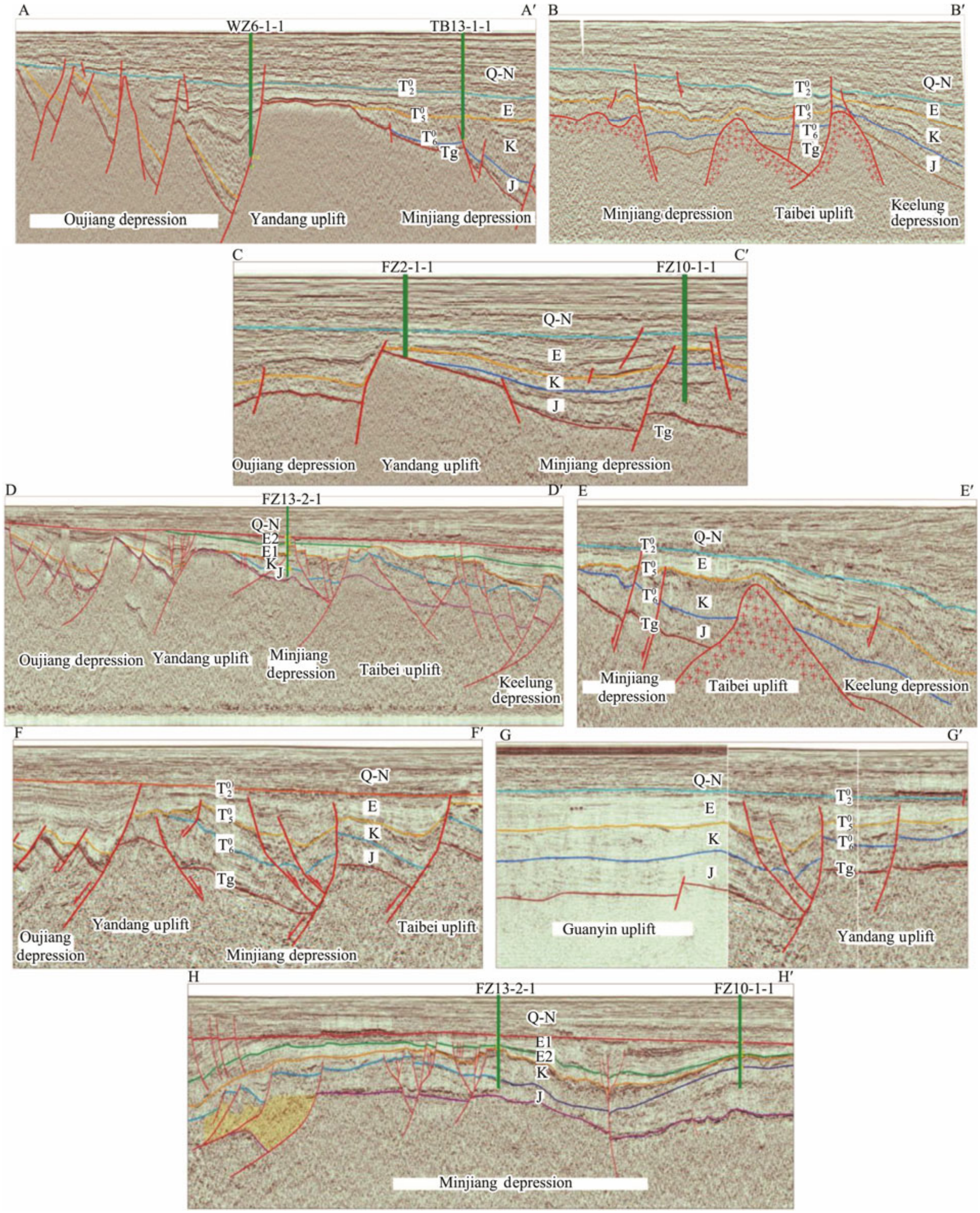

Fig.11 Seismic reflection profiles in the southern East China Sea (from Li *et al.*, 2012). Green vertical bars are the wells on the seismic lines. The locations of the profiles and wells are shown in Fig.2, and the labels at the bottom of the profiles are the names of the tectonic units. Labels Q-N, E, K and J are stratigraphic units separated by the main seismic reflectors (T_2^0, T_5^0, T_6^0 and T_g): Q-N, Quaternary and Neogene; E, Eogene (E1 and E2 represent the upper and lower parts, respectively); K, Cretaceous; and J, Jurassic.

The shelf area is covered by thick sediments. Because shallow volcanic intrusions are rare or small-scaled, the gravity and magnetic high anomalies should correspond to basement highs. However, the gravity anomaly reflects the undulation of the pre-Cenozoic basement, and the magnetic anomaly does not necessarily correspond to the variation of the basement. We suggest that a reasonable explanation for this discrepancy is the occurrence of Mesozoic strata that contains magmatic rocks. Through an analysis of seismic reflection profiles, Li *et al.* (2012) has proposed the existence of a Mesozoic Great East China Sea, which suggests that in the Mesozoic period, the Guanyin uplift and Taibei uplift did not exist and that the Yandang uplift was composed of three small discontinuous heaves. Therefore, the entire southern East China Sea shelf area displayed a continuous basin without alternatively arranged uplifts and depressions in the Mesozoic, and the basin might have extended southwestward and combined with the northern South China Sea shelf basin. Our results provide evidence from gravity and magnetic data to support this hypothesis.

Acknowledgements

This paper was funded by the National Key Basic Research Program of China (973 Program; Grant No. 2013CB429701) and National Natural Science Foundations of China (Grant Nos. 41206050 and 41202081). The authors wish to thank Professor F. Cai and research assistant C. S. Yang of QIMG for providing data. We would also like to thank senior engineer Z. X. Tian of QIMG for assistance in processing the data.

References

Bai, Y. L., Liu, Z., Zhang, Z. X., Yang, H. L., Zhang, G., Shi, Z. Y., and Du, R. L., 2010. Marine magnetic data processing technology and software realization. *Ocean Technology*, **29** (4): 34-37 (in Chinese with English abstract).

Chen, C. H., Lee, T., Shieh, Y. N., Chen, C. H., and Hsu, W. Y., 1995. Magmatism at the onset of back-arc basin spreading in the Okinawa Trough. *Journal of Volcanology and Geothermal Research*, **69**: 313-322.

Gao, D. Z., Hou, Z. Z., and Tang, J., 2000. Multiscale analysis of gravity anomalies on East China Sea and adjacent regions. *Chinese Journal of Geophysics*, **43** (6): 842-849 (in Chinese with English abstract).

Gao, D. Z., Zhao, J. H., Bo, Y. L., and Tang, J., 2006. A study on lithosphere 3D structures in the East China Sea and adjacent regions. *Chinese Journal of Geology*, **41** (1): 10-26 (in Chinese with English abstract).

Gao, D. Z., Zhao, J. H., Bo, Y. L., Tang, J., and Wang, S. J., 2004. A profile study of gravity-magnetic and seismic comprehensive survey in the East China Sea. *Chinese Journal of Geophysics*, **47** (5): 853-861 (in Chinese with English abstract).

Han, B., 2008. Geophysical field and deep tectonic features of East China Sea. PhD thesis. Institute of Oceanology, Chinese Academy of Sciences (in Chinese with English abstract).

Han, B., Zhang, X. H., and Meng, X. J., 2010. Magnetic field and basement features analysis in the east China Sea. *Marine Geology & Quaternary Geology*, **30** (1): 71-76 (in Chinese with English abstract).

Han, B., Zhang, X. H., Pei, J. X., and Zhang, W. G., 2007. Characteristics of crust-mantle in East China Sea and adjacent regions. *Progress in Geophysics*, **22** (2): 376-382 (in Chinese with English abstract).

Hirata, N., Kinoshita, H., Katao, H., Baba, H., Kaiho, Y., Koresawa, S., Ono, Y., and Hayashi, K., 1990. Report on DELP 1988 cruise in the southern Okinawa Trough, Part Ⅲ: Crustal structure of the southern Okinawa Trough. *Bulletin of the Earthquake Research Institute, University of Tokyo*, **66**: 37-70.

Honza, E., 1976. *Ryukyu Island (Nansei Shoto) Arc, GH75-1 and GH75-5 Cruises*. Geological Survey of Japan, Kawasaki-shi, 81pp.

Hou, C. S., Hu, J. C., Ching, K. E., Chen, Y. G., Chen, C. L., Cheng, L. W., Tang, C. L., Huang, S. H., and Lo, C. H., 2009. The crustal deformation of the Ilan Plain acted as a westernmost extension of the Okinawa Trough. *Tectonophysics*, **466**: 344-355.

Hsu, S. K., 2001. Magnetic inversion in the East China Sea and Okinawa Trough: Tectonic implications. *Tectonophysics*, **333**: 111-122.

Hsu, S. K., Sibuet, J. C., Monti, S., Shyu, C. T., and Liu, C. S., 1996. Transition between the Okinawa Trough backarc extension and the Taiwan collision: New insight on the Southernmost Ryukyu subduction zone. *Marine Geophysical Research*, **18**: 163-187.

Huang, C. Y., Chien, C. W., Yao, B. C., and Chang, C. P., 2008. The Lichi mélange: A collision mélange formation along early arcward backthrusts during forearc basin closure, Taiwan arc-continent collision. *The Geological Society of America, Special Paper*, **436**: 127-154.

Huang, H. H., Shyu, J., Bruce, H., Wu, Y. M., Chang, C. H., and Chen, Y. G., 2012. Seismotectonics of northeastern Taiwan: Kinematics of the transition from waning collision to subduction and postcollisional extension. *Journal of Geophysical Research*, **117** (B01313): 1-13.

Jiang, W. W., Liu, S. H., Hao, T. Y., and Song, H. B., 2002. Using gravity data to compute crustal thickness of East China Sea and Okinawa Trough. *Progress in Geophysics*, **17** (1): 35-41 (in Chinese with English abstract).

Jin, X. L., Yu, P. Z., Lin, M. H., Li, C. Z., and Wang, H. Q., 1983. Preliminary study on the characteristics of crustal structure in the Okinawa Trough. *Oceanologia et Limnologia Sinica*, **14** (2): 105-116 (in Chinese with English abstract).

Kimura, M., 1985. Back-arc rifting in the Okinawa Trough. *Marine and Petroleum Geology*, **2**: 222-240.

Klingelhoefer, F., Berther, T., Lallemand, S., Schnurle, P., Lee, C. S., Liu, C. S., McIntosh, K., and Theunissen, T., 2012. P-wave velocity structure of the southern Ryukyu margin east of Taiwan: Results from the ACTS wide-angle seismic experiment. *Tectonophysics*, **578**: 50-62.

Kodaira, S., Iwasaki, T., Urabe, T., Kanazawa, T., Egloff, F., Markris, J., and Shimamura, H., 1996. Crustal structure across the middle Ryukyu trench obtained from ocean bottom seismographic data. *Tectonophysics*, **263**: 39-60.

Lai, K. Y., Chen, Y. G., Wu, Y. M., Avouac, J. P., Kuo, Y. T., Wang, Y., Chang, C. H., and Lin, K. C., 2009. The 2005 Ilan earthquake doublet and seismic crisis in northeastern Taiwan: Evidence for dyke intrusion associated with on-land propagation of the Okinawa Trough. *Geophysical Journal International*, **179**: 678-686.

Lee, C. S., Shor Jr., G. G., Bibee, L. D., and Lu, R. S., 1980. Okinawa Trough: Origin of a back-arc basin. *Marine Geology*, **35**: 219-241.

Letouzey, J., and Kimura, M., 1985. Okinawa Trough genesis: Structure and evolution of a backarc basin developed in a continent. *Marine and Petroleum Geology*, **2**: 111-130.

Li, G., Gong, J. M., Yang, C. Q., Yang, C. S., Wang, W. J., Wang, H. R., and Li, S. Z., 2012. Stratigraphic feature of the Mesozoic 'Great East China Sea'–A new exploration field. *Marine Geology & Quaternary Geology*, **32** (3): 98-104 (in Chinese with English abstract).

Li, N. S., 1987a. Approaching the submarine faults of the Okinawa Trough on the basis of gravity data. *Marine Sciences*, **6**: 11-16 (in Chinese with English abstract).

Li, N. S., 1987b. On the fracturing structures of the Okinawa

Trough. *Oceanologia et Limnologia Sinica*, **19** (4): 347-358 (in Chinese with English abstract).

Li, W. R., Yang, Z. S., Zhang, B. M., and Wang, X. L., 1997. Study on the olivine of the southern Okinawa Trough. *Oceanologia et Limnologia Sinica*, **28** (6): 665-672 (in Chinese with English abstract).

Lin, J. Y., Hsu, S. K., and Sibuet, J. C., 2004a. Melting features along the Ryukyu slab tear, beneath the southwestern Okinawa Trough. *Geophysical Research Letter*, **31** (L19607): 1-4.

Lin, J. Y., Hsu, S. K., and Sibuet, J. C., 2004b. Melting features along the western Ryukyu slab edge (northeast Taiwan): Tomographic evidence. *Journal of Geophysical Research*, **109** (B12402): 1-15.

Lin, J. Y., Sibuet, J. C., and Hsu, S. K., 2005. Distributions of the east China Sea continental shelf basins and depths of magnetic sources. *Earth Planets Space*, **57**: 1063-1072.

Liu, G. D., 1992. *Geologic-Geophysics Features of China Seas and Adjacent Regions*. Science Press, Beijing, 248-271 (in Chinese with English abstract).

Liu, J. H., Wu, J. S., Fang, Y. X., and Wang, S. T., 2007. Pre-Cenozoic groups in the shelf basin of the East China Sea. *Acta Oceanologica Sinica*, **29** (1): 66-75 (in Chinese with English abstract).

Liu, Z., Bai, Y. L., Zhang, Z. X., Yang, H. L., Du, R. L., Shi, Z. Y., and Zhang, G., 2011. Marine magnetic data processing technology and software realization. *Marine Geology Frontiers*, **27** (9): 60-64 (in Chinese with English abstract).

Liu, Z., Zhao, W. J., Wu, S. G., Fan, F. X., and Sun, L. P., 2006. The basement tectonics in south of the Okinawa Trough. *Progress in Geophysics*, **21** (3): 814-824 (in Chinese with English abstract).

Ma, W. L., Wang, X. L., Jin, X. L., Chen, J. L., Han, X. Q., and Zhang, W. Y., 2004. Areal difference of middle and southern basalts from the Okinawa Trough and its genesis study. *Acta Geologica Sinica*, **78** (6): 758-769 (in Chinese with English abstract).

Park, J. O., 1998. Seiamic record of tectonic evolution and backarc rifting in the southern Ryukyu island arc system. *Tectonopgysics*, **294**: 21-42.

Rau, R. J., and Wu, F. T., 1995. Tomographic imaging of lithospheric structures under Taiwan. *Earth and Planetary Letters*, **133**: 517-532.

Shinjo, R., 1998. Petrochemistry and tectonic significance of the emerged late Cenozoic basalts behind the Okinawa Troughs Ryukyu Arc system. *Journal of Volcanology and Geothermal Research*, **80**: 39-53.

Shinjo, R., and Kato, Y., 2000. Geochemical constrains on the origin of bimodal magmatism at the Okinawa Trough, an incipient back-arc basin. *Lithos*, **54**: 117-137.

Sibuet, J. C., Deffontaines, B., Hsu, S. K., Thareau, N., Le Formal, J. P., and Liu, C. S., 1998. Okinawa Trough backarc basin: Early tectonic and magmatic evolution. *Journal of Geophysical Research*, **103** (B12): 30245-30267.

Sibuet, J. C., Letouzey, J., Barrier, F., Charvet, J., Foucher, J. P., Hilde, T. W. C., Kimura, M., Chiao, L. Y., Marsset, B., Muller, C., and Stephan, J. F., 1987. Back arc extension in the Okinawa Trough. *Journal of Geophysical Research*, **92** (B13): 14041-14063.

Sun, S. C., 1981. The Tertiary basin offshore Taiwan. *Proceedings of ASCOPE Conference and Exhibition*, Manila, Philippines, 126-135.

Teng, L. S., 1990. Geotectonic evolution of late Cenozoic arc-continent collision in Taiwan. *Tectonophysics*, **183** (1): 57-76.

Teng, L. S., 1996. Extensional collapse of the northern Taiwan mountain belt. *Geology*, **24** (10): 949-952.

Wang, C. S., Yang, M. L., Chou, C. P., Chang, Y. C., and Lee, C. S., 2000. Westward extension of the Okinawa Trough at its western end in the northern Taiwan area: Bathymetric and seismological evidence. *Terrestrial, Atmospheric and Oceanic Sciences*, **11** (2): 459-480.

Wang, K. L., Chung, S. L., Chen, C. H., Shinjo, R., Yang, T. F., and Chen, C. H., 1999. Post-collisional magmatism around northern Taiwan and its relation with opening of the Okinawa Trough. *Tectonophysics*, **308**: 363-376.

Wang, P., Liang, J. S., Zhao, Z. G., and Zhang, J. W., 2012. Diaoyu Islands folded – uplift belt evolution characteristics and its importance on the hydrocarbon exploration in East China Sea basin. *Petroleum Geology and Engineering*, **26** (6): 10-14 (in Chinese with English abstract).

Wang, T. K., Lin, S. F., Liu, C. S., and Wang, C. S., 2004. Crustal structure of the southernmost Ryukyu subduction zone: OBS, MCS and gravity modelling. *Geophysical Journal International*, **157**: 147-163.

Wu, S. G., Ni, X. L., and Guo, J. H., 2007. Balanced cross section for restoration of tectonic evolution in the southwest Okinawa Trough. *Journal of China University of Geosciences*, **18** (1): 1-10.

Wu, Z. Y., Wang, X. B., Jin, X. L., Li, J. B., and Gao, J. Y., 2004. The evidences of the backarc spreading and discussion on the key issues in the Okinawa Trough. *Marine Geology & Quaternary Geology*, **24** (3): 67-76 (in Chinese with English abstract).

Yang, C. Q., Yang, C. S., Li, G., Liao, J., and Gong, J. M., 2012a. Mesozoic tectonic evolution and prototype basin characters in the southern East China Sea shelf basin. *Marine Geology & Quaternary Geology*, **32** (3): 105-111 (in Chinese with English abstract).

Yang, C. S., Li, G., Yang, C. Q., Gong, J. M., and Liao, J., 2012b. Temporal and spatial distribution of the igneous rocks in the East China Sea shelf basin and its adjacent regions. *Marine Geology & Quaternary Geology*, **32** (3): 125-133 (in Chinese with English abstract).

Yang, Y. Q., Yang, C. Q., Li, G., and Gong, J. M., 2012c. Structure styles and their distribution pattern in the southern East China Sea shelf basin. *Marine Geology & Quaternary Geology*, **32** (3): 113-118 (in Chinese with English abstract).

Zhang, M. H., 2011. *Gravity, Magnetic and Electric Data Processing and Interpretation Software RGIS*. Geological Press, Beijing, 33-61 (in Chinese).

Zhao, J. H., 2004. The forming factors and evolvement of the Mesozoic and Cenozoic basin in the East China Sea. *Offshore Oil*, **24** (4): 6-14 (in Chinese with English abstract).

Zhao, Y. X., Liu, B. H., Li, X. S., Liu, C. G., Pei, Y. L., Wu, J. L., and Zheng, Y. P., 2009. Distributions of different submarine canyons on the East China Sea slop and their tectonic response. *Advances in Marine Science*, **27** (4): 460-468 (in Chinese with English abstract).

(Edited by Xie Jun)